Global NEST Journal, Vol 23, No 4, pp 572-580

Spatial and temporal variations of hydrodynamics and sediment dynamics in Indus River Estuary, Pakistan

Kalhoro N.A.[1,2,3]*, He Z.[1,2], Li L.[1, 2], Xu, D.[2], Jun W.[2], Zeb A.[3] and Khaskheli N.[1]

[1]Institute of Port, Coastal and Offshore Engineering, Ocean College, Zhejiang University, Hangzhou 310058, China

[2]State Key Laboratory of Satellite Ocean Environment Dynamics, Second Institute of Oceanography, State Oceanic Administration, Hangzhou 310012, China

[3]National Institute of Oceanography, Karachi75600, Pakistan

Received: 24/04/2020, Accepted: 21/10/2021, Available online: 10/12/2021

*to whom all correspondence should be addressed: e-mail: noorahmed_niopk@yahoo.com

https://doi.org/10.30955/gnj.003333

Graphical abstract

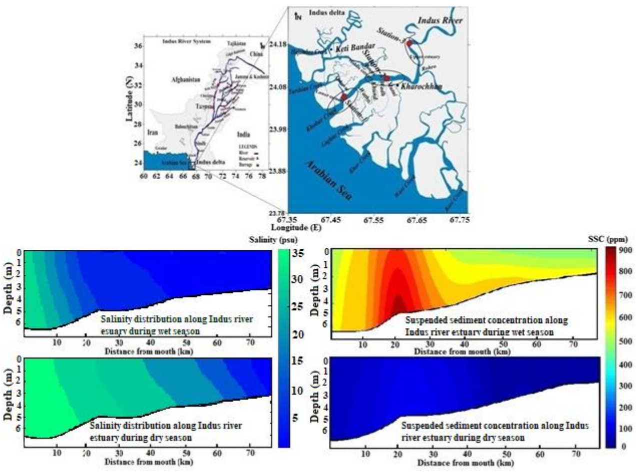

Abstract

Field investigations were conducted to study the seasonal variation of hydrodynamics and sediment transport in Indus River Estuary (IRE), Pakistan. The data of water levels, currents, salinity, and suspended sediment concentration (SSC) were collected hourly covering both wet and dry seasons. Tidal amplitudes were higher near the mouth than those at the middle and upper estuary. The ebb phase lasted longer than that of the flood during the wet season. The asymmetric tidal pattern with higher ebb velocity was observed during the wet season. A slight difference in current velocity was found during the dry season. The flood currents were higher at middle estuary than those in wet season. During the wet season, salinity variation within a tidal cycle slightly increased from the upper estuary to the mouth. Salinity was substantially higher during the dry season than the wet season at all three stations, with the absence of the flood-ebb variation, showing a strong saltwater intrusion. The suspended sediment concentration data revealed that the sediments were mainly brought into the estuary by freshwater discharge during the wet season. Sediment re-suspension process persists during the dry season, due to the tidal currents. A stronger saltwater intrusion occurred in the dry season due to weak river discharge. An estuarine turbidity maximum zone was formed near station-2 due to the combined effects of tides, river discharge and saltwater intrusion. Overall, field observations have shown a significant spatial and temporal variation in flood/ebb and wet/dry seasons for hydrodynamics and sediment transport in IRE.

Keywords: seasonality, fluvial discharge, hydrodynamics, SSC, saltwater intrusion, Indus River Estuary.

1. Introduction

Estuaries are the transitional zones between the land and marine environments. Any change in land (drainage basin) and marine environment affect the deltaic coast. Sea level rise and water usage in drainage basins are typical examples of such changes that may severely affect the coastline. Coastal erosion has been a world-wide problem in recent decades. It is estimated that over 32 years (1984-2015) about 28,000 km^2 coastal land has been eroded world-wide (Mentaschi *et al.,* 2018).

The increasing intensified human activities within river basin and along the coasts have aggravated the ongoing coastal erosion processes in many regions. However, decrease in sediment discharge from delta-forming rivers is a major cause of such erosion (Vinh *et al.,* 2016). At global scale, around 53 % of river sediment flux is now potentially trapped in reservoirs (Vörösmarty *et al.,* 2003). Sediment fluxes in many rivers, such as Mississippi, Indus, Yellow and Volta rivers have decreased by more than 60 % during recent decades, theses deltas are now threatened by coastline recession, because of insufficient sediment supply (Maloney *et al.,* 2018; Giosan *et al.*, 2014; Tessler *et al.,* 2015; Zang *et al.,* 2019).

In Asia, the rivers (Ganges, Brahmaputra, Yellow River, Yangtze, Mekong, Irrawady, Red River, Pearl River, Indus River) originating from the Tibetan plateau and the Himalayas were huge providers of sediments to the ocean, however, recent human activities have severely altered their sediment discharge, For example, in the Yellow River (Huanghe) sediment discharge decreased by 87% (from 1200 to 150× 10^6 t yr^{-1}) over a 40 year period (Wang *et al.,* 2008) and by 61% (from 119 to 46× 10^6 t yr^{-1}) in the Red River after the Hoa Binh dam settlement (Vinh *et al.,* 2014).

The construction of dams that supplies water for irrigation and hydro-power schemes is a common intervention in most rivers flowing through semi-arid areas (Ranasinghe *et al.,* 2019; GENZ *et al.,* 2008). Recent studies of 40 globally significant deltas show that more than 75% deltas are threatened by salt intrusion and coastal erosion (Ericson *et al.,* 2006).

The Indus River (IR) in Pakistan is one of the examples of irrigation developing system that resulting in a loss of water discharge and sediment load to the lower Indus River delta (Overeem and Syvitski, 2009). The Indus Deltaic region covers an area of approximately 1,000 square miles (Figure 1). It can be categorized as a dry (arid) tropical to subtropical deltas. The main source of freshwater and sediment to the delta was from the Indus River (IR) discharge. Indus Delta mainly received freshwater from IR during three months from July to September (wet season). It remained dry throughout the rest of the year (Inam *et al.,* 2007).

Up to about 50~70 years ago, there was a continuous supply of freshwater with an amount of185 BCM (billion cubic meters)/yr (Nasir and Akbar, 2012) and about 600 million tons of silt load annually, of which about 250 million tons used to reach Indus Delta (Wells and Coleman, 1984; Giosan *et al.,* 2006). The sediment load has now decreased to 13 million tons and river discharge was below the 10 MAF (million acre feet) per year (Syvitski *et al.,* 2014; Nasir and Akbar, 2012).

The reduction of freshwater discharge and sediment load in Indus River Delta started since the early 1960s, when several barrages were built along the river to feed one of the world's largest irrigation systems (Giosan *et al.,* 2006). The seasonal and annual river flows in the Indus River system are also variable (Warsi, 1991; Kijine *et al.,* 1992; Ahmad, 1993). According to Kalhoro *et al.* (2016), the wet season in Indus Delta persists for two months (August-September). The remaining period is associated with the dry season, when there is nearly no discharge below the Kotri barrage, the last barrage on Indus River. This huge shortage of water and sediment flux in Indus River has caused a significant reduction in the active delta. The deltaic shoreline along the central delta coast has started to recede at an average rate of about 50 m/year (Giosan*et al.,* 2006). Particularly, the mouth of the Indus Delta is the most eroded region. According to Kalhoro *et al.* (2016), a very high averaged erosion rate of ~179 m/year for the past 10 years was estimated in this region. The sea level rise along the Pakistan coast is recorded 1.1mm/year during past hundred years (Quraishee, 1988). Consequently, Indus Delta is now facing the serious threat due to climate change and anthropogenic activities continuing in the upstream of Indus River.

However, the available literature only describes the causes of reduction in freshwater and sediment supply below the Kotri barrage. The hydrodynamics and sediment dynamics in the Indus Delta have not been well understood due to the lack of proper field observations (Kravtsova *et al.,* 2009).

Hence, this study aims to study the hydrodynamics and sediment dynamics in the Indus River Estuary through field observation. Firstly, the temporal and spatial variability of tidal levels, currents, salinity and SSC is analyzed. Secondly, the impact of river discharge on tidal currents, salinity intrusion and estuarine turbidity maxima is examined.

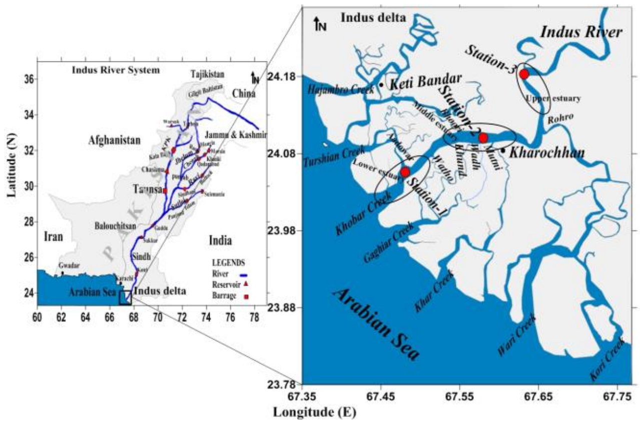

Figure 1. Study area and three monitoring sites at the lower, middle and upper estuary.

2. Methodology and study area

2.1. Study area

2.1.1. Indus river and its delta

Indus River is considered as one of the largest rivers in Asia with a drainage area of about 950,000 km^2. It originates from Tibetan Plateau near the Lake Mansarovar, then flows through Ladakh, Gilgit and Baltistan. It runs through the entire Pakistan and finally merges into the Arabian Sea near the port city of Karachi, Sindh Province of Pakistan (Figure 1). The length of the Indus River is around 2880 km (Abbasi, 2002). The Indus River Delta covers an area of 600,000 hectares (ha) from Korangi Creek in the north to Sir Creek in the south. It consists of 17 major creeks and many minor creeks, mud flats and fringing mangroves (Meynell and Qureshi, 1993).

The study area was the main channel of the Indus River Estuary (IRE), which is called Khobar Creek. The creek has a basin area of about 36 km^2.The Indus River Estuary is a bar-built estuary with a length of 40 km, comprising of 7 major tributaries, i.e. Rohro, Mutni, Wadh, Khund and Wathoto the southeast, while Bhoori and Aadowar to the southwest (Figure 1). It is classified as partially-mixed coastal plain estuary (Kalhoro *et al.,* 2016). The IRE is quite shallow with a maximum depth of 7 m. According to APN Report, 2004, sediments are relatively fine grained and mostly range between fine sand and clay, which are distributed in sand, silt and clay. The sand percentage was higher than that of both clay and silt. Clay was less than silt.

2.2. Data and methodology

Field work was conducted during the wet (September 2014) and dry (February-March 2015) seasons. There were three monitoring stations located at the lower, middle and upper Estuary, respectively, along the main river channel (Figure 1). Station-1 was located at the mouth of the estuary (lower estuary). Station-2 (middle estuary) was deployed at 20km upstream from the mouth, and Station-3 (upper Estuary) was located at about 40km upstream along the river channel.

Vertical profiles of salinity, SSC and current were measured hourly in 25 hours at all stations during both the wet and dry seasons. During the dry season (February-March 2015), the water level and turbidity data were also recorded hourly at station-2. In addition, a longitudinal profile of surface and near bed salinity and SSC was observed at every 5km from mouth up to 70 km upstream along the river during the wet (September) and dry (March) seasons. The longitudinal profiles of salinity and SSC were obtained from the mouth up to 70 km upstream along the river during the wet and dry seasons, respectively.

Water level and turbidity data were recorded every hour for 32 days with a pressure sensor based tidal gauge (RBR Model No.2050), fixed at the bottom near a fisherman floating jetty close to station-2. Currents were measured using a boat-mounted ADCP (Acoustic Doppler Current Profiler) with 1,200 kHz, at the Anchor stations. Water samples were obtained every hour at the surface and bottom levels, with a 5L Niskin bottle, inside the river to determine SSC values. SSC data were measured by filtering water samples with GF/F 0.7 µm filters and then dried by oven for 24 h at 60 °C. Salinity data were recorded using a water quality meter (Hydrolab Model MS-5) during survey period. Salinity sensor of water quality meter was calibrated through standard saline water.

The description of the field data was provided in Table 1.

Table 1. Descriptions of the field data

Field data	Observation time	Locations	Instruments
Sea surface level	25 hours in both wet and dry seasons; one month in dry season	Stations 1, 2 and 3	RBR Model No.2050
Current	25 hours in both wet and dry seasons	Stations 1, 2 and 3	ADCP 1200 kHz
Salinity	25 hours in both wet and dry seasons	Every 5 km along the river	Hydrolab Model MS-5
SSC	25 hours in both wet and dry seasons	Every 5 km along the river	Niskin bottles, GF/F 0.7 µm filters

3. Results

3.1. River flow and sediment load

The considered historical time series (monthly and yearly) of fluvial discharge and sediment load from the Kotri barrage hydrological station (Figure 2) revealed, the seasonal and annual river flows in the IRE system with a decreasing trend of fluvial discharge and sediment load below the Kotri barrage.

According to the yearly record of Kotri data, 118.77 BCM water with 274 MT sediment was released during 1973, while the discharge was only 0.32 BCM water with 1 MT of sediment in 2002 (Figure 2a). Monthly records over fifteen years indicated that Indus Delta receives fluvial discharge during the months of August and September, otherwise there is virtually no fluvial discharge below the Kotri barrage in the winter months. Figure 2b shows that the peaks of fresh water and sediment discharge during flood periods were also limited for short-term periods. The estuary remained dry during the rest of the year.

Thus, total annual river discharge was observed during the wet season (July to September) along the Indus Delta (Sindh Coast) spans, to the dry season (November to May) when river discharge is close to zero.

During the survey period, the monthly data of fluvial discharge obtained from the Executive Engineer Kotri Barrage revealed a total discharge of 2.58 BCM from March-2014 to March-2015. As shown in Figure 2c, about 97.7 % of the discharge (2.519 BCM) was recorded during July-September, 2014, while the rest of 10 months contributed only 2.3% of the discharge. For example, the total discharge of September was about 0.711BCM, while the discharge was around zero in March.

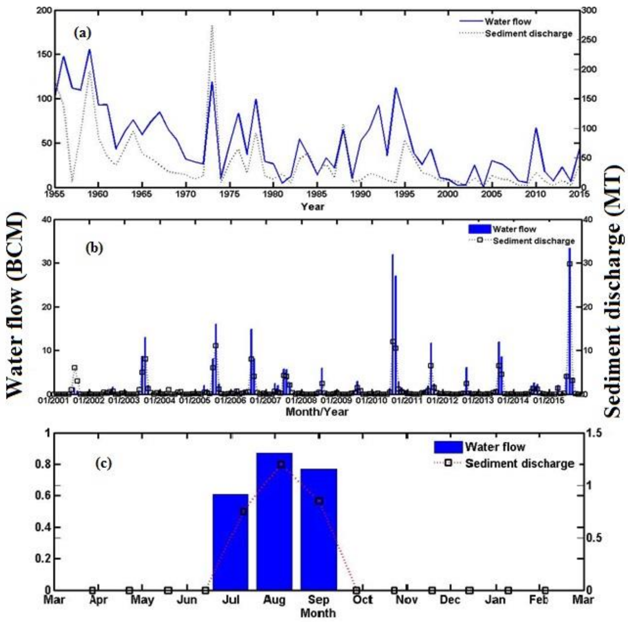

Figure 2. Yearly and monthly water flow and sediment discharge below the Kotri Barrage a (1955-2015), b (2000-2015) and c (March 2014-March 2015).

3.2. Tides and water currents

Tides along the Indus coast are semi-diurnal with two highs and two lows every day, but considerably vary from each other in tidal heights in daily tidal cycle, as shown in Figure 3. These are categorized as Higher High Water (HHW), Lower High Water (LHW), Higher Low Water (HLW) and Lower Low Water (LLW).

The tides observed at station-1 during the survey period showed maximum amplitude of 2.80 m and 2.40 m during the wet and dry seasons, respectively (Figure 3 a & b). Whereas, at station-2 the tidal level data show that the maximum amplitude was 2.56 m and 2.10 m during wet and dry season, respectively (Figure 3 c & d). The tidal range at station-1 (0.24 m) was larger than that at Kharochhan (station-2). It took about one hour for the tides to reach station-2 from station-1. The tidal amplitude at station-3 was 1.68 m and 1.52 m during wet and dry seasons respectively.

The current data were observed at the lower (near the mouth), middle and upper estuary, during both the wet and dry seasons. The current data showed strong spatial and temporal variation along the IRE.

During the wet season, the average river discharge was about 300.65 m^3s^{-1}. The maximum averaged current speed was 1.12 ms^{-1} and 1.32 ms^{-1} in flood phase and ebb phase, respectively, at the lower estuary (Figure 3a). The maximum current intensity was 1.2 ms^{-1} and 1.48 ms^{-1} during the flood tide and ebb tide, respectively. There were small vertical variations in surface and bottom currents intensity, as the estuary was shallow. Current speed of 0.62 ms^{-1} at the ebb phase and 0.58 ms^{-1} at the flood phase were recorded at the middle estuary (Figure 3c). The maximum current velocities were 0.43 ms^{-1} in flood phase and 0.54 ms^{-1} in ebb phase at the upper estuary (Figure 3e) with a small vertical variation.

During the dry season, when the river discharge was near zero, the maximum current intensities at the lower estuary were 0.98 ms^{-1} and 1.12 ms^{-1} in flood phase and ebb phase, respectively (Figure 3b). At the middle estuary, current intensities in the dry season were larger than those in the wet season, with the maximum current velocity of 0.72 ms^{-1} in the ebb phase and 0.75 ms^{-1} in the flood phase (Figure 3d). At the upper estuary (Figure 3f), the maximum current velocities were 0.51 ms^{-1} in flood phase and 0.53 ms^{-1} in ebb phase. The maximum current velocities were recorded before the peaks of the ebb and flood phases. Small difference was found in the near surface and near bed currents, as the estuary was shallow.

During the wet season, the ebb phase lasted longer than the flood phase, while no significant difference was found during the dry season. Small flood current intensity at the middle and upper estuary during the wet season indicated that during wet season flood tidal currents were lessened by the river runoffs. During the dry season, oceanic tides were dominated in the absence of river inflow. Therefore, the distance of saltwater intrusion in river channel was increased.

Temporally, during the dry season, small difference was observed in flood and ebb tides, compared with the wet season. The current velocities during the dry season were higher at station-2 than those observed in the wet season during flood phase and ebb phase, respectively. The minimum and maximum current velocities of 0.43 ms^{-1} and 1.12 ms^{-1} appeared at station-3 and station-1 (Figure 3f and b), respectively.

During the wet season, the flood current velocities at station-2 and station-3 were lessened by the river runoffs, however, in the absence of river runoffs in the dry season, flood current intensity was significantly higher (0.72 ms^{-1}) at middle and upper estuary, and seawater intruded further to upstream subsequently.

The tidal duration asymmetry was very weak. During the wet season, ebb phase lasted 2 hours longer than that of the flood phase. The current velocities were higher during the ebb at all three stations, because of the increased fluvial discharge. However, during the dry season, about one-hour phase difference was observed between flood and ebb phases.

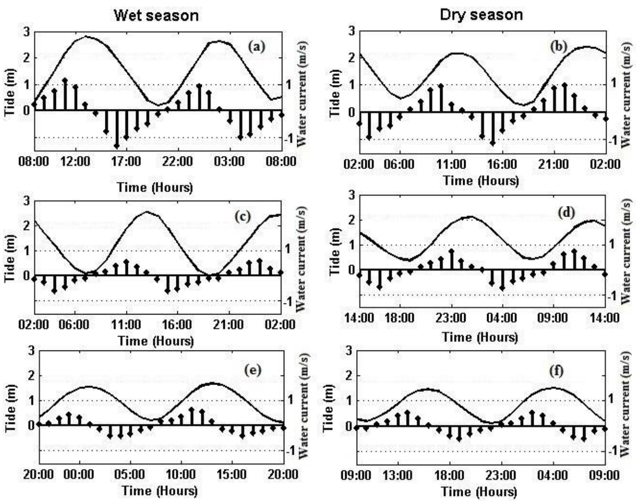

Figure 3. Hourly tides and water current velocities along IRE during wet (a, c, e) and dry (b, d, f) seasons.

3.3. Spatial and temporal variations in vertical salinity distribution

The hydrodynamic data shows strong spatial and temporal variations in tidal levels, and salinity distribution along the IRE.

Field observed data shows that at the mouth of the estuary (station-1), in one lunar month, the salinity varied from 7.95 to 33.04 PSU at the surface level and from 11.22 to 36.12 PSU at the bottom level, respectively. The variation of salinity in the flood-ebb tidal cycle was significant, with the minimum salinity value of 7.95 PSU during the ebb tide, and the maximum value of around 36.12 PSU during the floodtide. The surface to bottom salinity gradient was small. At the beginning of the flood phase, the whole water column was almost well mixed. However, when tidal advection decreased at the end of the flood phase, water column was slightly stratified due to density driven circulation.

At the other two stations (station-2 and 3), salinity was nearly absent during the ebb tide. The salinity at station-2 varied from 2.46 to 6.57 PSU at the surface level and from 2.88 to 7.53 PSU at the bottom level, respectively. At station-3, salinity varied from 1.2 to 2.5 PSU at the surface level and from 2 to 3 PSU at the bottom level, respectively. The flood-ebb variation was weak, because river discharge was dominant. The salinity in the estuary was strongly influenced by the periodicity of the fluvial discharge. The seawater plume was dispersed by river runoffs at about 8 km upstream, showing the well-mixed characteristics.

Salinity values showed strong seasonal variations. During the dry season, salinity data varied from 20 PSU to 37.10 PSU. The minimum and maximum value was observed at station-3 and station-1, respectively. During the dry season, flood/ebb and surface/bottom variation of salinity was weak at all stations (Figure 4 b, d & f), possibly due to the absence of river runoff.

The following Figure 5 was obtained by the three-dimensional (3D) Finite Volume Coastal Ocean Model (FVCOM) hydrodynamic model, Numerical results of salinity were compared with the field measured data, the field measurements were conducted during wet and dry seasons at eight stations along the channel.

The numerical results of salinity reveal that stratification/destratification occurs only at the mouth of IRE during the wet season. However, in the absence of fresh water discharge it is vertically homogenous and showed well mixed characteristics due to strong tidal forcing. Whereas during wet season it behaves as weakly stratified or partially mixed estuary result from tidal advection and weak river discharge. In the presence of fresh water, salinity was lower at ebb tides, while higher at flood tides when the whole water column filled with saline water. Whereas, the water column was partially stratified when tidal straining decreases; however, a slight variation of surface to bottom was observed during the both tidal phases, but it is more obvious during flood phase due to density difference (Figure 5a).

On the other hand, during the dry season, in the absence of fresh water discharge salinity was substantially higher; as a result, flood/ebb and vertical variation was absent (Figure 5b). Because, mixing processes in estuaries are mainly activated by tidal currents and freshwater discharge. The river runoff causes both downstream movement of the saline water and estuarine circulation; however, when runoff decreases the intensity of estuarine circulation decreases.

In stratified estuaries, salt transport predominantly due to advection by the net landward flow and the estuarine salt transport (Hansen *et al.,* 1966); however, in relatively well-mixed or weakly stratified estuaries, tidal dispersion plays an important role in the salt balance (Smith, 1980). Whereas, the combined effects of river discharge, tides, and topography control seawater intrusion into the estuaries.

However; IRE is quite shallow, the results indicate that the river runoff plays an important role in controlling the seawater intrusion. In the case of 300m^3/s fresh water discharge, vertical variation was not significant because the river runoff dispersed seawater plume at the mouth of estuary.

Figure 4a shows that during the wet season, though the difference of salinity from bottom to surface is small, an interface between saltwater and freshwater and the mixture between saltwater and freshwater are present during whole tidal cycle. However, in the absence of river discharge it changes from partially-mixed type circulation to a well-mixed type circulation. Simultaneously, the extent of the seawater intrusion into the estuary increases. Hence tides are the main dominant factor for seawater intrusion in IRE.

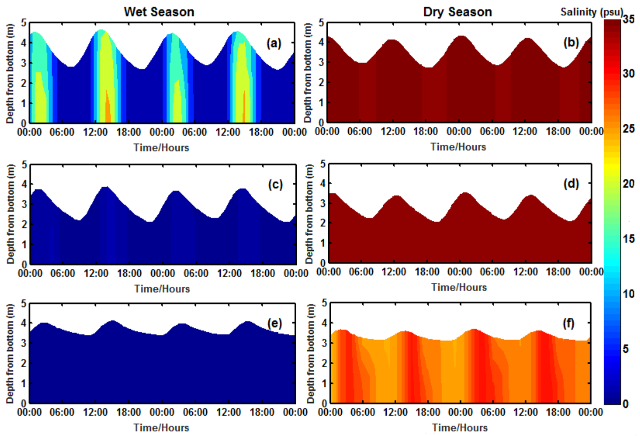

Figure 4. Hourly salinity (surface & bottom) variations at station-1,2 and 3 during the wet (a,c,e) and dry (b,d,f) seasons.

3.4. Spatial and temporal variations in SSC

According to the hourly variations, the SSC values were high at all stations during the wet season, due to the large amount of sediment load from the river.

Spatially, at station-1 (near the mouth), SSC values varied from 229.6 to 1192.5 ppm near the surface level and 492 to 1360 ppm near the bottom level, with a mean concentration of 733.224 ppm at the surface level and a mean concentration of 940.284 ppm near the bottom level (Figure 5a). At station-2, SSC values of 345.8 to 1233.5 ppm near the surface level and 512.3 to 1528.4 ppm near the bottom level were recorded (Figure 5c). The mean concentration was 886.856 ppm near the surface level and 1075.872 ppm near the bottom level. At station-3, SSC values varied from 331 to 515 ppm at the surface and 392 to 610 ppm near the bottom (Figure 5e).

Temporally, at station-1, the mean SSC value of 792.4 and 976.8ppm near the surface level and near the bottom level, respectively, was observed during the ebb tides. During the flood phase, the mean SSC was 669.1 and 900.75 ppm at the surface and bottom level, respectively (Figure 5b). At station-2, the mean SSC value of 870.4 and 1027.5ppm appeared at the surface and bottom level, respectively during flood phase. During ebb phase, the mean SSC was 904.7 and 1128.23 ppm at surface and bottom, respectively (Figure 5d). At station-3, the SSC values varied from 331 to 515 ppm at the surface during flood and 392 to 602 ppm near the bottom in ebb phase as shown in Figure 5f.

SSC data showed great variations in both seasons and tidal cycles. On one hand, the near surface and near bottom SSC values at all stations were about 10 times higher during the wet season than those during the dry season. This high SSC during the wet season was mainly contributed by river runoffs, which contained about 97% of river discharge of the whole year. The SSC at all sites had a phase lag comparing with the tidal level, but had a very close phase with the tidal current. The maximum SSC appeared immediately after the peak of current speed. On the other hand, the low SSC data had almost no difference from ebb to flood during the dry season. It was due to the local resuspension caused by tidal currents, as the maximum SSC occurred at the same time with the maximum current velocity.

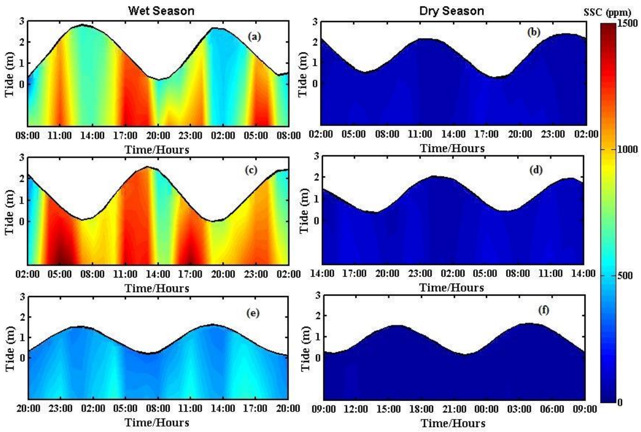

Figure 5. Hourly SSC (surface & bottom) variations at station-1, 2 and 3 during wet (a, c, e) and dry (b, d, f) seasons.

3.5. Longitudinal distribution of salinity and SSC

During the wet season, maximum salinity gradient was formed at station-1 at about 5km upstream, whereas 5 PSU salt wedge extended up to about 15 km upstream (Figure 6a). However, in the rest of the estuary, fluvial discharge was dominant and its salinity was nearly absent.

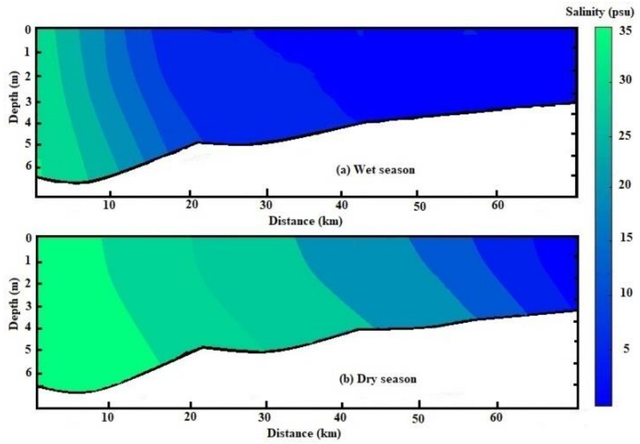

Figure 6. Water salinity distribution along IRE during wet (a) and dry (b) seasons.

During the dry season, the water column was well-mixed, and the longitudinal salinity intrusion was stronger than that in the wet season. Thus, 35 PSU salt wedge intruded to about 15 km upstream, and 25 PSU salinity plume reached about 40 km upstream (Figure 6b). Horizontal salinity gradient, generated and advected during flood tides in many tidal channels, filled the lower estuary with marine water. As a result, the increased volume of saline water strengthened the tidal pumping towards upstream. The horizontal density gradient varies from the mouth to upstream, while vertical variation was absent. In the absence of river runoffs, estuarine density driven circulation was not significant.

During the wet season, the horizontally distribution of SSC values along the estuary varied from 229.6 to 1233.5 ppm near the surface level, and 392 to 1475 ppm near the bottom level. The minimum value was observed at station-1 (near mouth), while maximum SSC occurred in the estuarine turbidity maximum (ETM) at station-2, as shown in Figure 7a.

During the dry season, SSC values varied from 63.71 to 136.90 ppm and only slight variation was observed during ebb/flood phases. The maximum values were recorded at about 20-25 km upstream, which showed the existence of ETM (Figure 7b).

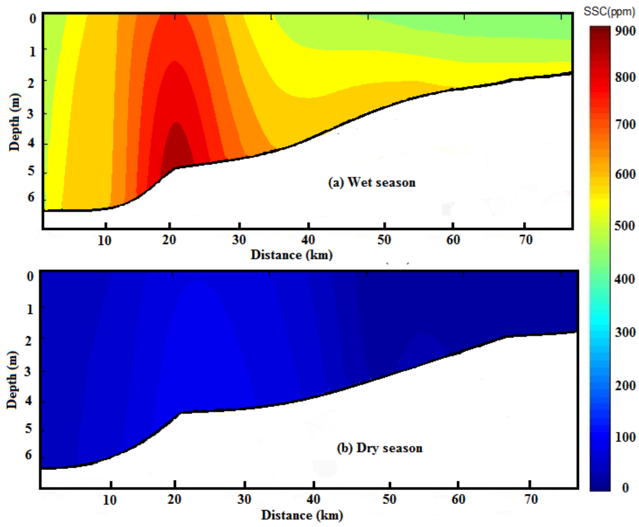

Figure 7. SSC distribution along the IRE during the dry (a) and wet (b) seasons.

The sediment sizes mostly ranged between fine sand and clay size (APN report, 2004) and appeared not at the mouth, but at the middle estuary. The distribution pattern of sediment revealed that the tidal forcing had pushed the ETM in the Indus River Estuary back to upstream.

During dry season, in the absence of river flow, clay and silt sediments were higher at upstream. They had been deposited and re-suspended by tidal actions. During the dry season, a salinity front reached station-2, indicated by a salinity of almost zero PSU. The stratified water at the front of the salinity intrusion inhibited the turbulent mixing, and consequently caused the suspended sediment to sink and the subsequent formation of the ETM. Therefore, sediment trapping might take place near station-2, where a saltwater wedge existed.

An ETM zone was observed to move backward and forward near station-2 (between 20 km and 25 km) between the dry and wet seasons, due to the combined effects of tidal forcing and river discharge. The vertical gradient of SSC was much larger during the wet season than that during the dry season. The stratification caused by salinity and SSC in the dry season was stronger than that in the wet season.

4. Discussion

4.1. Asymmetric variations of hydrodynamics and sediment dynamics

Our field observation at the three stations clearly shows the asymmetric seasonal variations and flood-ebb characteristics in hydrodynamics and sediment dynamics in the Indus River Estuary.

Monthly river flow data revealed that freshwater runoff was limited in wet seasons (July-September), while drought occurred in the rest of time. The sediment loads from the Indus River showed an asymmetric variation that similar as the river discharge.

The tidal levels and currents data revealed that the ebb phase was dominated with a considerably longer duration and higher current velocity than the flood phase at all stations in the wet season, as the ebb velocity was enhanced by the freshwater discharge. The flood-ebb asymmetry became stronger from the upstream to the mouth of the estuary, as can be seen at station-1. This agreed with the previous literatures of Morales (1993) and Lobo *et al.* (2004), who reported that ebb currents are faster than flood especially at the lower estuary. In the dry season, the tidal asymmetry in the estuary was weak, because the river discharge was nearly zero and the hydrodynamics was mainly controlled by tides. The flood and the ebb current periods were nearly equal at all the three stations from the mouth to the upstream.

The turbidity and SSC values showed asymmetric seasonality due to the river discharge and sediment load. The flood-ebb asymmetry also occurred to the turbidity and SSC values, due to tidal variation.

4.2. Estuarine stratification

During the wet season, the hourly variation of salinity revealed that the water column near the mouth (station-1) was always weakly stratified. The stratification decreased when the flood flow reached its peak value, due to tidal mixing and tidal straining. Similar trend was observed by Vaz *et al.* (2005) in the Vouga River Estuary. This is also in agreement with Siegle *et al.* (2009), who reported that tidal propagation enhances estuarine mixing. Lower salinity with small vertical variation was observed at stations 2 and 3, due to the sufficient freshwater discharge. The salinity plume in the estuary was pushed out by the high freshwater discharge. Hence, salinity near the mouth was nearly absent during ebb tides. This agrees with Zhang and Deng (2010), who stated that river flow in the Pearl River Estuary was an important factor to reduce the distance of salinity intrusion.

During the dry season, salinity in the Indus River Estuary was substantially higher due to the lack of freshwater discharge, as well as strong tides. A well-mixed vertical profile occurred at station-1. The same pattern was observed at stations 2 and 3, which indicated that the estuary is mainly occupied by the seawater during dry seasons. However, a slight stratification was found between station 1 and 3, which might be caused by the small discharge from agricultural lands or seepage.

4.3. Variability of ETM zone

The SSC data showed great variations in both seasons and tidal cycles. On one hand, the SSC values at the surface and near the bottom at all stations during the wet season were about 10 times higher than with those during the dry season. This high SSC during the wet season is mainly contributed by river runoffs, which contains about 97% of river discharge of the whole year. The SSC at all sites has a phase lag comparing to the tidal level, but has a very close phase with the tidal current. The maximum SSC appears immediately after the peak of current reaches. On the other hand, the low SSC with slight difference from ebb to flood during the dry season is due to the local resuspension caused by tidal currents, because the maximum SSC occurs at the same time with the maximum current velocity; meanwhile, there is no flow from river. The SSC peak appears not at the mouth, but at the location about 20 km away from the mouth to the upstream, which reveals that the estuarine maximum turbidity in the Indus River Estuary has been pushed back by the tidal forcing. Therefore, sediment trapping might take place in the middle estuary, where a week saltwater wedge also exists.

5. Conclusions

Our study illustrates that the hydrodynamics and sediment dynamics of the Indus River Estuary is largely depend on the freshwater input variability during wet and dry seasons. Consequently, the seasonality of fluvial discharge results in substantial variations of salinity and SSC. During dry seasons, seawater intrusion becomes more serious and more frequent, resulted from the imbalance between river discharge and tidal propagation. The observed data shows that the salinity in the IRE increases during dry seasons, when the upstream runoff decreases, and vice versa.

During wet seasons, the ebb tidal phase is dominated with a longer duration and higher current velocity than the flood phase at all stations, due to the sufficient river discharge released to the estuary. On the other hand, tidal symmetry was observed in both tidal levels and currents during the dry season. Tidal forcing together with zero river discharge intruded to a longer distance towards upstream.

The investigation indicates that the estuary exhibits weakly stratified or partially mixed characteristics at station-1 near the mouth during wet seasons. Fresh and turbid water was dominated in the middle and upper estuary, respectively. In contrast, salinity was significantly higher with a maximum of 37 PSU during dry seasons, when upstream fluvial discharge is near zero. Meanwhile, the flood/ebb and vertical variation was weak at all stations, which show the well-mixed characteristics. The SSC data denote that the sediments are mainly transported to estuary during the wet season when freshwater is discharged from the Indus River. Local re-suspension processes persist during dry seasons. The ETM is observed not at the mouth, but about 20 km away from the mouth to the upstream, which might cause sediment trapping in the middle estuary where saltwater wedge also exists. Hence, the anthropogenic activities in the upstream, especially serious reduction of fresh water and runoff regulation, have greatly affected the hydrodynamics and the associated sediment transport in the Indus River Estuary.

Acknowledgements

The authors thank the financial support from the State Key Laboratory of Satellite Ocean Environment Dynamics, Second Institute of Oceanography, Ministry of Natural Resources of China, Zhejiang University of China and the National Institute of Oceanography of Pakistan. This study is supported by the National Key Research and Development Program of China (2017YFC1405100), the National Natural Science Foundation of China (11672267), the Zhejiang Provincial Natural Science Foundation of China (LR16E090001) and the Fund of China-Pakistan Joint Research Center Joint Laboratory of China.

References

Abbasi A.G. (2002), Restoration of Sindh's Primary Rights over River Indus, *18th Convention of SANA,* Cherry Hill, New Jersey, July 4–7.

Ahmad N. (1993), *Water Resources of Pakistan*, Lahore.

APN, report. (2004), An assessment of nutrient, sediment and carbon fluxes to the coastal zone in South Asia and their relationship to human activities, 1–359.

Ericson J.P., Vörösmarty C.J., Dingman S.L., Ward L.G. and Meybeck M. (2006), Effective sea-level rise and deltas: causes of change and human dimension implications. *Global and Planetary Change,* **50**, 63–82.

Genz F., Lessa G.C. and Cirano M. (2008), Vazaomínima para estuarios: um estudo de caso no Rio Paraguaçu/BA. RevistaBrasileira de RecursosHidricos. v. 13, p. 73–82.

Giosan L. and Syvitski J. (2014), Constantinescu, S.; Day, J. Protect the world's deltas. *Nature*, **516**, 31–33.

Giosan L., Constantinescu S., Clift P.D., Tabrez A.R., Danish M. and Inam A. (2006), Recent morphodynamics of the Indus delta shore and shelf. *Continental Shelf Research*, **26**, 1668–1684.

Inam A., Clift P.D., Giosan L., Tabrez A.R., Tahir M., Rabbani M.M. and Danish M. (2007), *The Geographic, Geological and Oceanographic Setting of the Indus River*. Large Rivers: Geomorphology and Management, Edited by A. Gupta, John Wiley & Sons, Ltd, 333–346.

Kalhoro N.A., He Z., Xu D., Faiz M., Lv, Y., Sohoo N. and Bhutto A.H. (2016), Vulnerability of the Indus River Delta of the North Arabian Sea, Pakistan, *Global NEST Journal*, **18**(3), 599–610.

Kijine J.W., Jr E.J. and Van der Velde. (1992), *Irrigation Management Implications of Indus Basin Climate Change - Case Study*. Lahore: IIMI.

Kravtsova V.I., Mikhailov V.N. and Efremova N.A. (2009), Variations of the hydrological regime, morphological structure and landscapers of the Indus River delta (Pakistan) under the effect of large-scale water management measures, *Water Resources*, **36**(4), 365–379.

Lobo J., Plaza F., Gonzales R., Dias J., Kapsimalis V., Mendes I., and Rio V.D. (2004), Estimations of bedload sediment transport in the Guadiana Estuary (SW Iberian Peninsula) during low river discharge periods. *Journal of Coastal Research*, **41**(Special Issue), 12–26.

Maloney J.M., Bentley S.J., Xu, K., Obelcz J., Georgiou I. and Miner M. (2018), Mississippi river subaqueous delta is entering a stage of retrogradation. *Marine Geology*, **400**, 12–23.

Mentaschi L., Vousdoukas M.L., PekelF., Voukouvalas E. and Feyen L. (2018), Global long-term observations of coastal erosion and accretion. *Scientific Reports*, 1–11.

Meynell P. and Qureshi T. (1993), Sustainable management of mangroves in the Indus Delta, Pakistan. Towards the Wise Use of Wetlands, in David, T. (Ed.), *Ramsar Bureau, Gland*, 113–22.

Morales J.A. (1993), *Sedimentology del Estuario del Guadiana* (S.W. Espantilde;a-Portugal). Ph.D. Thesis, University of Sevilla, Sevilla, Spain, 274.

Nasir, S.M. and Akbar G. (2012), Effect of River Indus flow on low riparian ecosystems of Sindh: a review paper, *Records Zoological Survey of Pakistan*, 21, 86–89.

Overeem I. and Syvitski J.P.M. (2009), *Dynamics and Vulnerability of Indus delta systems*. GKSS Research Center LOICZ International Project Office Institute for Coastal Research, Germany, 1–56.

Quraishee G.S. (1988), Global Warming and Rise in Sea Level in the South Asian Seas Region, in the Implication of Climatic Changes and the impact of rise in Sea level in the South Asian Seas Region, 1–21.

Ranasinghe R., Wu C.S., Conallin J., Duong T.M., & Anthony E.J. (2019), Disentangling the relative impacts of climate change and human activities on fluvial sediment supply to the coast by the world's large rivers: Pearl River Basin, China. *Scientific Reports*, **9**(1), 9236. https://doi.org/10.1038/s41598-019-45442-2.

Siegle E., Schettini C.A.F., Klein A.H.F. and Toldo Jr E.E. (2009), Hydrodynamics and suspended sediment transport in the Camboriu Estuary – Brazil: Pre-Jetty conditions. *Brazilian Journal Oceanography*, **57**(2), 123–135

Syvitski J.P.M., Kettner A.J., Overeem P., Giosan L., Brakenridge G.R., Hanon M. and Bilham R. (2014), Anthropocene Metamorphosis of the Indus Delta and Lower Floodplain. http://dx.doi.org/10.1016/j.ancene

Tessler Z.D., Vörösmarty C.J., Grossberg M., Gladkova I., Aizenman H., Syvitski J.P., Foufoula-Georgiou E. (2015), Profiling risk and sustainability in coastal deltas of the world. *Science*, **349**, 638–643.

Vaz N., Dias J.M. and Martins I. (2005), Dynamics of a temperate fluvial estuary in early winter. *Global, Nest*, 1–7.

Vinh V.D., Ouillon S., Tanh T.D. and Chu L.V. (2014), Impact of the Hoa Binh dam (Vietnam) on water and sediment budgets in the Red River basin and delta, Hydrol. *Earth System Science*, **18**, 3987–4005.

Vinh V.D., Ouillon S., Thao V.N. and Tien N.N. (2016), Numerical simulationsof suspended sediment dynamics due to seasonal forcing in the Mekong coastal area. *Water*, (8) 2–23.

Vörösmarty C.J., Meybeck M., Fekete B., Sharma K., Green P. and Syvitsk J.P.M. (2003), Anthropogenic sediment retention: Major global impact from registered river impoundments. *Global and Planetary Change*, **39**, 169–190.

Wang H.J., Yang Z.S., Wang Y., Saito Y. and Liu J.P. (2008), Reconstruction of sediment flux from the Changjiang (Yangtze River) to the sea since the 1860s, *Journal of Hydrology*, **349**, 318–332.

Wars M. (1991), Indus and Other River Basin of Pakistan, Stream Flow Records, Case Study Report. WAPDA.

Wells J.T. and Coleman J.M. (1984), Deltaic morphology and sedimentology, with special reference to the Indus River delta. In: Haq B.U., Milliman J.D. (Eds.), Marine Geology and oceanography of Arabian Sea and Coastal Pakistan. Van Nostrand Reinhold Company, New York, 85–100.

Zhang X. and Deng J. (2010), Affecting Factors of Salinity Intrusion in Pearl River Estuary and Sustainable Utilization of Water Resources in Pearl River Delta. Springer Science B.V., 1-8.

Zang Z.C., Xue Z.G., Xu K.H., Bentley S.J., Chen Q., D' Sa E.J., Ge Q. (2019), A Two Decadal (1993-2012) Numerical Assessment of Sediment Dynamics in the Northern Gulf of Mexico, *Water*, **11**, 938.